1-1-2010

Cosmogenic 21Ne analysis of individual detrital grains: opportunities and limitations

Alexandru T. Codilean
University of Glasgow, codilean@uow.edu.au

Paul Bishop
University of Glasgow

Trevor B. Hoey
University of Glasgow

Finlay M. Stuart
Scottish Universities Environmental Research Centre

Derek Fabel
University of Glasgow

Cosmogenic 21Ne analysis of individual detrital grains: opportunities and limitations

Abstract

We use a numerical model describing cosmogenic nuclide acquisition in sediment moving through the upper Gaub River catchment to evaluate the extent to which aspects of source area geomorphology and geomorphological processes can be inferred from frequency distributions of cosmogenic 21Ne (21Nec) concentrations in individual detrital grains. The numerical model predicts the pathways of sediment grains from their source to the outlet of the catchment and calculates the total 21Nec concentration that each grain acquires along its pathway. The model fully accounts for variations in nuclide production due to changes in latitude, altitude and topographic shielding and allows for spatially variable erosion and sediment transport rates. Model results show that the form of the frequency distribution of 21Nec concentrations in exported sediment is sensitive to the range and spatial distribution of processes operating in the sediment's source areas and that this distribution can be used to infer the range and spatial distribution of erosion rates that characterise the catchment. The results also show that lithology can affect the form of the 21Nec concentration distribution indirectly by exerting control on the spatial pattern of denudation in a catchment. Model results further indicate that the form of the distribution of 21Nec concentrations in the exported sediment can also be affected by the acquisition of 21Nec after detachment from bedrock, in the diffusive (hillslope) and/or advective (fluvial) domains. However, for such post-detachment nuclide acquisition to be important, this effect needs to at least equal the nuclide acquisition prior to detachment from bedrock.

Keywords

cosmogenic nuclide analysis, landscape evolution, numerical modelling, sediment provenance, Namibia, GeoQuest

Disciplines

Medicine and Health Sciences | Social and Behavioral Sciences

Publication Details

Codilean, A. T., Bishop, P., Hoey, T. B., Stuart, F. M. & Fabel, D. (2010). Cosmogenic 21Ne analysis of individual detrital grains: opportunities and limitations. Earth Surface Processes and Landforms, 35 (1), 16-27.

Cosmogenic ^{21}Ne analysis of individual detrital grains: Opportunities and limitations

Short title: Cosmogenic ^{21}Ne analysis of individual detrital grains

Alexandru T. Codilean[†,⋆],

Paul Bishop[†], Trevor B. Hoey[†], Finlay M. Stuart[§], and Derek Fabel[†]

† Department of Geographical & Earth Sciences, The University of Glasgow,
Glasgow G12 8QQ, UK
Tel: +44 (0) 141 330 4782, Fax: +44 (0) 141 330 4894

§ Isotope Geosciences Unit, Scottish Universities Environmental Research Centre (SUERC),
East Kilbride G75 0QF, UK
Tel: +44 (0) 135 522 3332, Fax: +44 (0)135 522 9898

⋆Corresponding author: tibi.codilean@ges.gla.ac.uk

Abstract

We use a numerical model describing cosmogenic nuclide acquisition in sediment moving through the upper Gaub River catchment to evaluate the extent to which aspects of source area geomorphology and geomorphological processes can be inferred from frequency distributions of cosmogenic ^{21}Ne ($^{21}Ne_c$) concentrations in individual detrital grains. The numerical model predicts the pathways of sediment grains from their source to the outlet of the catchment and calculates the total $^{21}Ne_c$ concentration that each grain acquires along its pathway. The model fully accounts for variations in nuclide production due to changes in latitude, altitude and topographic shielding and allows for spatially variable erosion and sediment transport rates. Model results show that the form of the frequency distribution of $^{21}Ne_c$ concentrations in exported sediment is sensitive to the range and spatial distribution of processes operating in the sediment's source areas and that this distribution can be used to infer the range and spatial distribution of erosion rates that characterise the catchment. The results also show that lithology can affect the form of the $^{21}Ne_c$ concentration distribution indirectly by exerting control on the spatial pattern of denudation in a catchment. Model results further indicate that the form of the distribution of $^{21}Ne_c$ concentrations in the exported sediment can also be affected by the acquisition of $^{21}Ne_c$ after detachment from bedrock, in the diffusive (hillslope) and/or advective (fluvial) domains. However, for such post-detachment nuclide acquisition to be important, this effect needs to at least equal the nuclide acquisition prior to detachment from bedrock.

Keywords: cosmogenic nuclide analysis, landscape evolution, numerical modelling, sediment provenance, Namibia.

Introduction

The last two decades in geomorphology have seen a re-emergence of research into the links between large-scale tectonic processes and long-term landscape evolution (Bishop, 2007). Part of the reason for this re-emergence has been the realisation that surface processes can play a key role in moderating tectonics, and possibly climate, through the isostatic response of

the crust to sediment loading and denudational unloading (Molnar and England, 1990; Molnar, 2003). There is thus a heightened need for improving our understanding of how surface processes operate and how landscapes respond to these surface processes. This need in turn requires the development of techniques and methodologies that enable unravelling the 'history' of landscapes by quantifying rates of landscape change and sediment fluxes over the relevant spatial and temporal scales. This paper examines some opportunities and limitations of the analysis of the frequency distribution of terrestrial cosmogenic nuclide concentrations (TCNs) in general, and cosmogenic ^{21}Ne concentrations in particular, in individual grains in a sedimentary deposit as a method for unravelling aspects of source area geomorphology and geomorphological processes.

TCNs (both stable and radioactive) are produced by the interaction of cosmic rays with minerals in the upper few metres of the surface of the Earth. Several nuclides, in particular ^{3}He, ^{10}Be, ^{21}Ne, ^{26}Al, and ^{36}Cl, are now routinely measured and have been used in geomorphological studies for the last two decades (Bierman, 1994; Bierman and Nichols, 2004; von Blanckenburg, 2005). TCNs can detect landscape changes over timescales of the order of $10^3 - 10^6$ years. Further, the production of TCNs is confined to the upper few metres of the Earth's surface, and the production rates of these nuclides are highly sensitive to elevation (Lal, 1991). The latter means that the total TCN concentration acquired by a grain, before being detached from bedrock, is sensitive to variations in bedrock erosion rate (i.e., how long the grain spends within the upper few metres of the Earth's surface) and to changes in surface elevation.

TCN concentrations in alluvial sediment are now routinely used to estimate time- and space-averaged catchment-wide denudation rates, but have the potential to offer considerably more. Each individual sediment grain has a unique history as it is eroded from the parent material, and then transported via hillslope processes into the fluvial network and through this network to the point of sampling (Figure 1). Grains accumulate TCNs prior to their detachment and throughout all stages of their transport and storage, so long as they are not deeply buried or shielded. Just as the TCN concentration of a grain reflects its history of erosion and transportation, so the frequency distribution of TCN concentrations in a large number of grains leaving a catchment should reflect the geomorphological character and history of the catchment. Thus, the frequency distribution of nuclide concentrations in exported sediment has the potential to provide not only a mean erosion rate but also a signature of the

range and spatial distribution of erosion rates across a catchment.

Of the currently used nuclides, cosmogenic ^{3}He ($^3\mathrm{He_c}$) and cosmogenic ^{21}Ne ($^{21}\mathrm{Ne_c}$) are the most suitable for determining the frequency distribution of nuclide concentrations in sediment. This is because (1) extraction and determination of both $^3\mathrm{He_c}$ and $^{21}\mathrm{Ne_c}$ is relatively straightforward and inexpensive allowing for a large number of individual measurements, and (2) small sample sizes are required, allowing $^3\mathrm{He_c}$ and $^{21}\mathrm{Ne_c}$ to be measured in individual pebbles (Niedermann, 2002). Further, $^3\mathrm{He_c}$ and $^{21}\mathrm{Ne_c}$ are stable and do not decay with time, and so in principle their use is not limited to modern sediment (cf. Libarkin *et al.*, 2002). Measurements of $^3\mathrm{He_c}$ in alluvial olivine grains from the Waimea River catchment on the island of Kauai, Hawaii (Gayer *et al.*, 2008) and of $^{21}\mathrm{Ne_c}$ in individual alluvial quartz pebbles from the upper Gaub River catchment in central-western Namibia (Codilean *et al.*, 2008) have confirmed the practicability of both $^3\mathrm{He_c}$ and $^{21}\mathrm{Ne_c}$ analyses in individual detrital grains, demonstrating (1) that the spatial non-uniformity of erosion rates in a catchment is reflected in the frequency distribution of TCN concentrations in sediment leaving the catchment, and (2) that the form of this distribution is sensitive to the range of erosion rates in the catchment.

In this study we use a GIS-based numerical model to explore the sensitivity of the form of the TCN concentration distribution in sediment leaving the upper Gaub River catchment to (i) sample size, and (ii) assumptions about the characteristics of the sediment's source areas. This sensitivity analysis aims to identify the factors that control the form of the frequency distribution of single grain TCN concentrations, and therefore, tests the potential of frequency distributions of single grain TCN concentrations for inferring aspects of source area geomorphology. The poor retentivity of $^3\mathrm{He_c}$ in quartz, the favored target mineral for exposure age and erosion rate studies, limits the applicability of this nuclide and so this study focuses only on $^{21}\mathrm{Ne_c}$. Nevertheless, the methodology presented here is readily adaptable for $^3\mathrm{He_c}$. Furthermore, the conclusions of this study are valid for any TCN, with the caveat that, in the case of radio-nuclides, loss of nuclides through radioactive decay may lead to equifinal TCN concentration distributions and so can hinder the interpretation of results. A description of the study catchment and a summary of published cosmogenic nuclide data for this catchment are presented, followed by an outline of the theoretical background of the numerical model, a description of the structure and implementation of the model, and the results of the sensitivity analysis.

Study area

The upper Gaub River catchment, with an area of ∼1200 km^2, is a tributary of the Kuiseb River (∼15,500 km^2), one of the major ephemeral river systems draining western Namibia (Figure 2). The geomorphology of the upper Gaub is that of a high elevation passive margin (Ollier and Marker, 1985; Summerfield, 1991) with an extensive low-relief upland region and a dissected, high-relief zone marking the Great Escarpment (Figure 3A). The catchment elevation ranges from 949 m at the outlet to 2351 m on the Gamsberg massif.

Catchment lithology is complex and the principal rock units belong to four different groups: pre-Rehoboth, Rehoboth (1650−1860 Myr), Sinclair (1050−1400 Myr), and Damara (650−850 Myr) (Ziegler and Stoessel, 1993; Becker *et al.*, 1994, 1996). Of these groups, however, only two (Rehoboth and Sinclair) occupy large areas of the catchment (Figure 3B). The Rehoboth Sequence consists of low- to medium-grade metamorphosed quartzites and schists, ortho-amphibolites, anorthosites and serpentinites. These rocks have been intruded by granitoids of Rehoboth age, and by granites belonging to the Sinclair Sequence. The pre-Rehoboth units occur in the south of the study area and consist of low- to medium-grade quartzites, schists and greenschists and medium- to high-grade migmatic gneisses, amphibolites, quartzites and schists. The Damara Sequence is exposed in the north and consists of metasedimentary rocks. Quartz is an abundant component of all lithological units and crops out throughout the catchment.

Denudation rates in central-western Namibia are overall very low, with the steeper escarpment area eroding more rapidly than either the more gently sloping coastal plain or the upland plateau (Figure 4A). Cosmogenic nuclide-based bedrock erosion rates average around 2.5 m·Myr^{-1} on the coastal plain and upland plateau (Bierman and Caffee, 2001; van der Wateren and Dunai, 2001); the steeper escarpment area is eroding in the proximity of the study catchment at a rate of around 7.9 m·Myr^{-1} (Cockburn *et al.*, 2000). Denudation rates based on cosmogenic ^{10}Be analysis of sediment are higher than their bedrock counterparts but exhibit a similar regional pattern: 6.4 and 5.8 m·Myr^{-1} on the coastal plain and upland plateau respectively, and 12.9 m·Myr^{-1} on the escarpment (Bierman and Caffee, 2001; Codilean *et al.*, 2008). The measured catchment-wide denudation rates show a strong linear correlation with source catchment mean slope (Figure 4B). This strong linear relationship between denudation

rate and slope is consistent with the findings of Ahnert (1970), Milliman and Syvitski (1992), Summerfield and Hulton (1994), and Harrison (2000) who identified catchment relief (a proxy for mean catchment slope) as a dominant control on rates of denudation and the associated development of topography.

Numerical model

The objective of the numerical modelling exercise is to test the potential of frequency distributions of single grain $^{21}Ne_c$ concentrations for inferring aspects of source area geomorphology. The model is used heuristically (cf. Oreskes *et al.*, 1994) to explore the sensitivity of the form of the frequency distributions of single grain $^{21}Ne_c$ concentrations to sample size and characteristics of the sediment's source areas.

Theoretical background

Consider the case of a sediment grain sampled at a catchment outlet (Figure 5). The $^{21}Ne_c$ concentration of this grain depends on the grain's source location in the catchment, and its pathway through the catchment. As erosion and the removal of overlying material brings rocks closer to the surface, bedrock enters the zone where the intensity of penetrating cosmic radiation is sufficient to react with the target elements. At this point the production of cosmogenic isotopes commences and then increases exponentially as the rock moves to the surface. The production of $^{21}Ne_c$ at a given depth $P(z)$ is given by:

$$P(z) = P(0) \exp\left[-z/z^*\right] \tag{1}$$

where $P(0)$ is the production rate at the surface (atoms·g^{-1}·yr^{-1}), z^* (e-folding length) is the ratio between the absorption mean free path for nuclear interacting particles in the target ($\Lambda = 145 - 160$ g·cm^{-2}) and the density of the target (ρ, g·cm^{-3}), and z is depth (cm) (Lal, 1991). $P(0)$ is mainly a function of altitude, geomagnetic latitude (Lal, 1991; Dunai, 2000; Stone, 2000) and exposure geometry (Dunne *et al.*, 1999; Codilean, 2006). $P(0)$ also varies with changes in the intensity of the cosmic flux through time (Gosse and Phillips, 2001), but this variability can be neglected in areas, such as the Gaub, where denudation rates are very

low (Desilets and Zreda, 2003; Dunai, 2000; Lifton *et al.*, 2005). $P(0)$ is given by:

$$P(0) = P_{\mathrm{SLHL}} \prod_{i=1}^{n} C_{sf}(i) \tag{2}$$

where P_{SLHL} is the surface production rate at sea level and high latitudes ($P_{\mathrm{SLHL}}[^{21}\mathrm{Ne_c}] = 19.0 \pm 3.7$ atoms·g^{-1}·yr^{-1}; Niedermann, 2000) and $\prod_{i=1}^{n} C_{sf}(i)$ is the product of all relevant scaling factors.

The number of atoms of $^{21}\mathrm{Ne_c}$ that are acquired *in situ* by the grain, prior to detachment (1 in Figure 5), is a function of the bedrock erosion rate (ε) during the time taken for the grain's host rock to move from ∼2 m depth to the surface. Under steady continuous erosion, the number of atoms of $^{21}\mathrm{Ne_c}$ that are acquired prior to detachment ($N_{21\mathrm{Ne}}(\mathbf{r})$) is given by (Lal, 1991):

$$N_{21\mathrm{Ne}}(\mathbf{r}) = \frac{P(0)z^*}{\varepsilon} \tag{3}$$

Equation (3) applies to both rock surfaces and mixed regolith as long as erosion is continuous and steady, and it does not depend on the thickens of the regolith layer (Granger *et al.*, 1996; Granger and Riebe, 2007). That is, the cosmogenic $^{21}\mathrm{Ne_c}$ concentration in eroding regolith is the same as at the surface of eroding bedrock, independent of the thickness of the regolith layer.

Following detachment, the acquisition of $^{21}\mathrm{Ne_c}$ by a sediment grain depends on the geomorphic processes in the catchment. Material movement on hillslopes can be conceptualised as a transport layer of finite thickness Z, where this thickness can be expressed as a function of z^* so that $\beta(\mathbf{c}) = [Z/z^*(\mathbf{c})]$, with $\mathbf{c}$ standing for colluvium (Repka *et al.*, 1997). The number of $^{21}\mathrm{Ne_c}$ atoms acquired by a stationary grain on the hillslope, for a certain period of time, is given by:

$$N_{21\mathrm{Ne}}(\mathbf{c}) = P(0)T \int_{0}^{Z \text{ where } Z=\beta(\mathbf{c})z^*(\mathbf{c})} \exp[-z/z^*(\mathbf{c})]\vartheta(z)dz \tag{4}$$

where T is time (years) and $\vartheta(z)$ is a function describing the probability of the grain being located at a certain depth within the transport layer (Repka *et al.*, 1997). Assuming that $\vartheta(z)$

is uniform with depth, equation (4) reduces to:

$$N_{21\mathrm{Ne}}(\mathbf{c}) = P(0)T\frac{1-\exp[-\beta(\mathbf{c})]}{\beta(\mathbf{c})} \tag{5}$$

This equation further reduces to equation (3) in the case of thick deposits ($Z > 2z^*(\mathbf{c})$) (Granger *et al.*, 1996; Repka *et al.*, 1997). In order to obtain the total $^{21}\mathrm{Ne_c}$ concentration acquired by a grain subject to diffusive transport processes, equation (5) is integrated with elevation and yields:

$$N_{21\mathrm{Ne}}(\mathbf{c}) = \int_{h_{\mathrm{out}}}^{h_{\mathrm{in}}} P(0)(h)T(h)\frac{1-\exp[-\beta(\mathbf{c})]}{\beta(\mathbf{c})}dh \tag{6}$$

where h_{in} stands for the elevation at which the grain is detached from the parent material and h_{out} stands for the elevation at which the grain is transferred to the fluvial system. Both $P(0)$ and T are expressed as functions of elevation (h), and $\beta(\mathbf{c})$ is assumed constant with elevation. Specifying $P(0)$ and T as functions of elevation is non-trivial, requiring knowledge of the transport velocity of grains at all elevations, including periods of storage. Transport velocity in turn requires knowledge of the dominant processes operating at different elevations and slopes within the catchment. Finally, the assumption of perfect mixing may not hold, particularly where the regolith is deep and some grains may be stored at depths greater than $2z^*(\mathbf{c})$ (cf. Crozier *et al.*, 1990).

Once grains enter the fluvial system, the mode of transport changes to being purely advective, although with considerable storage potential in some situations. Equations (4), (5), and (6) can be adapted for the fluvial case in which the depth of the transport layer is defined as $\beta(\mathbf{f}) = [Z/z^*(\mathbf{f})]$, with $\mathbf{f}$ standing for fluvial. Perfect vertical mixing can be assumed, although this is a simplification in rivers with a wide range of coarse grain sizes (cf. Hassan and Church, 1994). Rather than attempting to incorporate the details of size sorting in the fluvial system, problems arising as a result of assuming perfect vertical mixing can be avoided by restricting the grain sizes that are sampled for $^{21}\mathrm{Ne_c}$ analyses. Thus, the number of atoms of $^{21}\mathrm{Ne_c}$ that are acquired while the grain passes through the fluvial system is given by:

$$N_{21\mathrm{Ne}}(\mathbf{f}) = \int_{h'_{\mathrm{out}}}^{h'_{\mathrm{in}}} P(0)(h)T(h)\frac{1-\exp[-\beta(\mathbf{f})]}{\beta(\mathbf{f})}dh \tag{7}$$

where h'_{in} stands for the elevation at which the grain enters the fluvial system and h'_{out} stands for the elevation at which the sample was taken at the catchment outlet. Summation of equations (3), (6) and (7) gives the total number of atoms of $^{21}\mathrm{Ne_c}$ acquired by a given sediment grain.

Model implementation and structure

Integrating the acquisition of $^{21}\mathrm{Ne_c}$ both in time and in space over evolving terrains over long time periods is complex. As an approximation, equations (3), (6) and (7) are implemented in a two dimensional GIS-based numerical model that assumes elevation to be constant through time. This simplification is reasonable given that the timescales of nuclide acquisition during bedrock erosion and sediment transport are short relative to the timescale of landscape evolution and so the changes in landscape morphology and elevation while a grain acquires cosmogenic nuclides during bedrock erosion and transport are negligible. Moreover, the numerical model is used heuristically to explore 'what if' questions (cf. Oreskes *et al.*, 1994), and the GIS-based implementation is adequate for such use.

The model works by predicting the pathways of sediment grains from their source to the outlet of the catchment. The pathway of each grain, obtained using the D8 flow routing algorithm (O'Callaghan and Mark, 1984; Jenson and Domingue, 1988), is divided into three conceptual domains: a bedrock domain, a hillslope domain, and a fluvial domain (Figure 5). The sum of the $^{21}\mathrm{Ne_c}$ acquired in each domain yields the total $^{21}\mathrm{Ne_c}$ acquired by the grain. A probabilistic sampling approach is used to simulate the effects of a spatially variable quartz flux that may be the result of spatially variable erosion and/or lithology.

The $^{21}\mathrm{Ne_c}$ acquired by a grain in the bedrock domain (Figure 5) is calculated using equation (3) with the scaling factors of Dunai (2000) and Codilean (2006). Bedrock erosion (ε) is allowed to be either spatially uniform or spatially variable (e.g., as a linear function of slope). The $^{21}\mathrm{Ne_c}$ acquired by a grain in any DEM cell in the hillslope and fluvial domains (Figure 5) depends on the elevation of the cell, the depth at which the grain is buried within the transport

layer, and the length of time the grain spends crossing the cell. No vertical movement of the grains during transport over a cell is assumed and the $^{21}Ne_c$ concentration acquired at a given cell ($N_{21Ne}(\mathbf{c,f})_i$) is obtained from:

$$N_{21Ne}(\mathbf{c,f})_i = P(0)_i T_i \exp[-z(\mathbf{c,f})_i / z^*(\mathbf{c,f})] \tag{8}$$

where i refers to cell i, $z(\mathbf{c,f})_i$ is the depth at which the grain is buried within the transport layer (controlled by a linear random function; $0 < z(\mathbf{c,f})_i < z(\mathbf{c,f})_{max}$, where $z(\mathbf{c,f})_{max}$ is the maximum depth of the transport layer), and T_i is the time (years) spent crossing cell i. $z^*(\mathbf{c,f})$ is varied as a function of the porosity of the sediment in the transport layer. T_i depends on the 'virtual' velocity ($m \cdot yr^{-1}$) of downstream sediment movement and is calculated differently depending on whether the cell is part of the hillslope domain or part of the fluvial domain. Observations from a 15 m resolution ASTER satellite image and slope-area data for the study catchment suggest that in this catchment the transition between the hillslope and fluvial domains occurs at a threshold catchment area of $\sim 5 \times 10^4$ m^2 (cf. Montgomery and Foufoula-Georgiou, 1993).

For a hillslope cell, i, the virtual velocity of downstream sediment movement, $v(\mathbf{c})_i$, is approximated by:

$$v(\mathbf{c})_i \propto K_D / z(\mathbf{c})_i \tag{9}$$

where K_D is a diffusion coefficient ($m^2 \cdot yr^{-1}$) (Beaumont *et al.*, 1992; Kooi and Beaumont, 1994). Given the thin regolith mantle in the Gaub River catchment, the model treats the transport of hillslope materials as a slow quasi-continuous diffusive process, neglecting the effect of landsliding on cosmogenic nuclide acquisition (e.g., Niemi *et al.*, 2005). Because $v(\mathbf{c})_i$ incorporates both intervals of movement and rest, K_D has to be seen as a sediment movement virtual velocity regulator rather than the classic Fickian diffusion coefficient considered in other studies (e.g., Martin and Church, 1997).

For a DEM cell, i, flagged as channel, the virtual velocity of sediment, $v(\mathbf{f})_i$, depends on local channel slope, water discharge, mean bed sediment size, and storage. Ferguson *et al.* (2002) derived the following equation for virtual velocity:

$$v_j = a\,(g d_j)^{0.5}\,\tau_*^b \exp\left(\frac{-c d_j}{\overline{d}}\right) \tag{10}$$

in which subscript j refers to grain size j, g is acceleration due to gravity ($\mathrm{m{\cdot}s^{-2}}$), τ_* is dimensionless shear stress and a, b, and c are empirical coefficients. Considering mean grain size $\overline{d} = d_j$, equation (10) can be expressed as:

$$v_m = k\left(\overline{d}\right)^{0.5}\tau_*^b \tag{11}$$

in which k combines the constant parts of all terms in equation (10) and m refers to the velocity of the mean grain size. $\overline{d}$ can be expressed as a function of the maximum mean bed material size in the headwaters, d_{max} (m), so that:

$$\overline{d} = d_{max}\exp(-\alpha x) \tag{12}$$

where α is a downstream fining coefficient and x is the flow path distance from the channel head (km) (Krumbein, 1937). α is calculated as:

$$\alpha = 1/\sqrt{A_{\mathbf{Tot}}} \tag{13}$$

where $A_{\mathbf{Tot}}$ is total drainage area ($\mathrm{km^2}$) (Hoey and Bluck, 1999). Dimensionless shear stress can be expressed as (Chang, 1988, p.39):

$$\tau_* = HS/1.65 d_j \tag{14}$$

where H is flow depth and is expressed as a function of discharge using a standard hydraulic geometry equation: $H = cQ^f$, where c and f are empirical parameters. Assuming that $Q = RA$ where R is rainfall (taken as uniform across the catchment) and A is drainage area, $H = cR^f A^f = c'A^f$. Thus $v(\mathbf{f})_i$ can be approximated as:

$$v(\mathbf{f})_i \propto [d_{max}\exp(-\alpha x)]^{1-b}\left(A_i^f S_i\right)^b \zeta \tag{15}$$

where A_i is drainage area upstream of cell i (m^2), S_i is local channel gradient ($m \cdot m^{-1}$), b is an empirical constant, and ζ is a slow-down coefficient to account for episodic sediment transport in ephemeral channels. The value of f incorporates a generic increase in channel width with discharge, and is generally accepted to be $\sim$0.5 (Whipple and Tucker, 1999). Ferguson *et al.* (2002) found $b = 0.85$. Although equation (15) accounts for intervals of both movement and rest, it neglects long-term sediment storage. This simplification is justified in the Gaub by the absence of any sizeable colluvial aprons, terraces or floodplains that might store sediment for significant periods.

Sensitivity analysis

The GIS-based model is used to explore the sensitivity of the $^{21}Ne_c$ concentration distribution in the sediment leaving the upper Gaub River catchment to the number of sediment grains in a sample and to the assumptions that are made about the characteristics of the sediment's source areas, specifically, spatial patterns of denudation, post-detachment sediment residence times, and lithology.

Number of grains in a sample

In each of the simulations intended for exploring the sensitivity of the $^{21}Ne_c$ distributions to the number of grains in a sample, the parameters of the GIS-based model were set to reflect the conditions in the upper Gaub River catchment, namely, spatially-variable erosion that is linearly proportional to slope and negligible $^{21}Ne_c$ acquisition after detachment from bedrock (Bierman and Caffee, 2001; Codilean *et al.*, 2008).

Codilean et al. (2008) have shown that the form of the frequency distribution of $^{21}Ne_c$ in the sediment leaving a catchment is sensitive to the range of erosion rates in the catchment. However, the precision of model results depends on the number of grains that are in a sample (Figure 6) and so the latter also affects the power with which the form of the $^{21}Ne_c$ distribution can discriminate between different ranges of bedrock erosion rates. As shown in Figure 7 (inset), the distribution of the predicted $^{21}Ne_c$ curves within the envelopes is not uniform. This means that despite having overlap between the $^{21}Ne_c$ distribution envelopes predicted

for different ranges of bedrock erosion rates, in principle it is still possible to discriminate between them with a certain degree of confidence. In Figure 7 for example, despite having the 32 measured $^{21}Ne_c$ concentrations lie within the predicted $^{21}Ne_c$ distribution envelopes for the three ranges of bedrock erosion rates, the model results show that it is unlikely that the 32 measured $^{21}Ne_c$ concentrations are the result of bedrock erosion rates ranging between either 0.1 and 5 m·Myr^{-1} or between 0.1 and 15 m·Myr^{-1}. These results suggest that it should in principle be possible to use the distribution of $^{21}Ne_c$ in exported sediment to infer the range of erosion rates responsible for the production of that sediment even for the relatively small sample size of 32 clasts.

Spatial pattern of denudation

In a catchment that is in topographic steady-state (i.e., bedrock erosion is uniform throughout the catchment) and with negligible post-detachment nuclide acquisition, the frequency distribution of $^{21}Ne_c$ mirrors the distribution of elevation values in the catchment, because of the strong dependence of nuclide production on altitude (cf. Lal, 1991; Figure 8A). Deviation from topographic steady-state conditions results in changes in the form of the $^{21}Ne_c$ distribution due to non-uniform production of sediment throughout the catchment. If erosion is proportional to slope, steeper areas erode more rapidly and contribute a greater proportion, relative to their surface area, of the sediment leaving the catchment. Moreover, this more rapid erosion means that the resultant sediment will have relatively low nuclide concentrations, skewing the distribution of $^{21}Ne_c$ concentrations leaving the catchment toward lower values.

The results in Figure 8 very clearly show that the form of the $^{21}Ne_c$ distribution is highly sensitive to the pattern of spatial variability of the different erosion rates present in a catchment. In particular, this analysis of detrital $^{21}Ne_c$ concentrations demonstrates that, in the Gaub, the relationship between bedrock erosion and slope is not non-linear (Figure 8B).

Post-detachment sediment residence times

Sediment grains can acquire $^{21}Ne_c$ after detachment from bedrock while moving through the colluvial and fluvial systems. Thus, at least theoretically, two end-member cases may be identified in accounting for the $^{21}Ne_c$ concentrations in the sediment leaving a catchment

(Figure 9). One end-member case assumes that virtually all the $^{21}Ne_c$ is acquired prior to detachment (pre-detachment dominated) and the measured $^{21}Ne_c$ concentrations can be interpreted in terms of denudation rates (Figure 9A). The other end-member case assumes that pre-detachment $^{21}Ne_c$ acquisition is negligible relative to that acquired during transport, in which case the $^{21}Ne_c$ concentrations are post-detachment dominated and are interpreted in terms of sediment residence (or exposure) times rather than denudation rates (Figure 9B).

In a post-detachment dominated case (Figure 10), the $^{21}Ne_c$ concentration distributions in the sediment are not primarily determined by catchment hypsometry. If long-term sediment storage in channels is not significant, the forms of these distributions will depend mainly on the spatial distribution of the locations (both in terms of distance and travel time) of the sediment grains' source areas relative to the nearest sediment delivery arteries (i.e., channels). If river networks are considered as space-filling (cf. Tarboton *et al.*, 1988; La Barbera and Rosso, 1989), the frequency distribution of the distances from sediment grain source locations to the nearest sediment delivery arteries will always be highly skewed toward the shorter distances (Figure 11). Consequently, the form of $^{21}Ne_c$ distributions in catchments with very slow diffusive sediment transport rates will always exhibit a distribution of TCN concentrations that is highly skewed toward lower values (reflecting the higher frequency of shorter colluvial transport distances).

The skew of the 'post-detachment dominated' distributions (Figure 10) is similar to that obtained by Codilean *et al.* (2008) for the 32 Gaub pebbles, and it could be argued that the form of the measured $^{21}Ne_c$ distribution is a signature of post-detachment-dominated conditions in the Gaub rather than of the spatial variation in erosion rates. However, a post-detachment-dominated case requires that the post-detachment-acquired $^{21}Ne_c$ in the sediment grains is at least equal to or greater than the $^{21}Ne_c$ that was acquired prior to the detachment of the grains from bedrock. For this to apply in the Gaub, post-detachment sediment residence times would need to be of the order of $10^5 - 10^6$ years. Given the small catchment size and lack of accommodation space, such long sediment residence times are unrealistic for the Gaub (cf. Dosseto *et al.*, 2008).

Lithology

Non-uniform distribution of quartzose lithologies in a catchment affects the frequency distribution of $^{21}Ne_c$ in the sediment leaving the catchment in at least two ways: (1) via the proportion of quartz contributed by different parts of the catchment to the total mix at the outlet, and (2) via the $^{21}Ne_c$ concentration that is acquired by grains prior to detachment. The latter is the result of differential lithological resistance to erosion. The former is the result of either differential quartz concentrations in the various catchment lithologies or differential bedrock erosion (as a result of differential lithological resistance to erosion) or a combination of both. Two scenarios are considered here: (i) where lithology controls only the proportion of quartz contributed by different parts of the catchment (i.e., the various lithologies have different concentrations of quartz but erode at a similar rate); and (ii) where lithology controls both the proportion of quartz contributed by different parts of the catchment and the spatial pattern of bedrock erosion.

The study catchment consists of four different lithological units: pre-Rehoboth, Rehoboth, Sinclair, and Damara (Ziegler and Stoessel, 1993; Becker *et al.*, 1994, 1996; Figure 3). The pre-Rehoboth, Rehoboth, and Damara units consist predominantly of quartzites and the Sinclair unit is predominantly granite. Thus, for the purposes of the sensitivity analysis, the catchment is divided into two zones: quartzites and granites (zones 1 and 2 in Figure 12A1, respectively). This breakdown of lithology into two zones −quartzites and granites− is simplistic but appropriate for the type of questions that are considered here.

Figure 12A2 shows the results of scenario (i) (i.e., lithology controls only the proportion of quartz contributed by different parts of the catchment). The erosion rates in the two lithological zones are set to be equal ($\varepsilon 1 = \varepsilon 2$) and zone 1 (quartzites) is set to contribute more quartz to the total than zone 2 (granites). Scenario (i) yields $^{21}Ne_c$ distributions that are almost identical to each other and that mirror the form of the hypsometric curve (Figure 12A2), indicating that the form of the $^{21}Ne_c$ distribution is not sensitive to the proportion of quartz contributed by different parts of the catchment to the total mix at the outlet. In scenario (ii) (lithology controls both the proportion of quartz and the spatial pattern of bedrock erosion) the erosion rate in zone 1 is set to be 20% higher than that in zone 2, and just as in scenario (i), zone 1 is se to contribute more quartz to the total than zone 2. Scenario

(ii) yields $^{21}Ne_c$ distributions that are only subtly different to those obtained for scenario (i) (Figure 12A3). To test whether this lack of sensitivity is due to the configuration of the two zones − zone 1 encompassing almost the entire range of elevations, and so $^{21}Ne_c$ production rates (Figure 12A1) − or whether it is more general, scenarios (i) and (ii) were run with two different zones: zone 1 consisting of the steep escarpment area plus the coastal plain and zone 2 consisting of the high elevation upland plateau (Figure 12B1). Using the same initial conditions as above (Figure 12A) yields $^{21}Ne_c$ distributions for the new zones (Figure 12B1) that are similar to those obtained before (Figures 12B2 and B3). Only when setting the erosion rate in zone 1 to be $> 50\%$ higher than that in zone 2 do the obtained $^{21}Ne_c$ concentration distributions become substantially different from each other and the hypsometric curve (Figure 12B4). These results suggest that (1) the form of the $^{21}Ne_c$ concentration distribution is not sensitive to the proportions with which the different catchment lithologies contribute quartz to the sediment sample at the outlet, and (2) the form of the $^{21}Ne_c$ concentration distribution is affected by the lithological make-up of the catchment only indirectly, if lithology exerts a substantial control on the spatial pattern of bedrock erosion rates.

Concluding discussion

The sensitivity analyses show that the form of the frequency distribution of $^{21}Ne_c$ concentrations in exported sediment is sensitive to the range and spatial distribution of processes operating in the sediment's source areas and that this distribution can be used to infer aspects of source area geomorphology. Notably, our data and modelling show that the source area characteristics that can be inferred from detrital TCN data include the range of erosion rates that characterise the catchment, with, in principle, a probability attached to that inference, even for the relatively small sample size of 32 clasts (Figure 7). TCN analyses of larger numbers of detrital grains potentially permit the determination of the probable range of erosion rates in the source area catchment with higher confidence. Thus, if sediment source catchment area is known, it should in principle be possible to use detrital TCN concentrations to determine the range of erosion rates responsible for the production of that sediment, complementing the more 'traditional' sedimentological tools for analysis of source area and sediment transport, including composition and textural maturity. Such determinations of course re-

quire assumptions (for example, the relationship between mean slope and erosion rate) and can be confounded by equifinal solutions flowing from variations in mean slope angle and an unknown (or imprecisely known) relationship between mean slope and erosion rate (cf. Figure 8B). These difficulties, however, can be alleviated by testing the assumptions *a priori* with $^{21}Ne_c$ analyses in a few additional carefully selected bedrock and/or sediment samples. Our results (and published data) show that the assumption of a linear relationship between mean slope and erosion rate is acceptable, but the ways in which other relationships between mean slope and erosion rate interact with varying slope angles in generating TCN concentrations in detrital grains deserve more attention.

Our results also show that the form of the frequency distribution of $^{21}Ne_c$ concentrations is insensitive to the non-uniform spatial distribution of quartzose lithologies in the catchment, thereby giving confidence that catchment-averaged erosion rates are not overly compromised by spatially non-uniform distributions of the target lithology(ies) for TCN analysis. Lithology may affect the form of the TCN concentration distribution indirectly, however, by exerting control on the spatial pattern of denudation in a catchment.

The form of the distribution of $^{21}Ne_c$ concentrations in the exported sediment can also be affected by the acquisition of $^{21}Ne_c$ after detachment from bedrock, in the diffusive (hillslope) and/or advective (fluvial) domains. However, for post-detachment nuclide acquisition to be important, this effect would need at least to equal the nuclide acquisition prior to detachment from bedrock. Codilean et al.'s (2008) $^{21}Ne_c$ data show no evidence of substantial post-detachment nuclide acquisition in the Gaub. Further, Carretier *et al.* (2009) have found, using a numerical model of alluvial sediment transport, that with a background bedrock erosion rate of 10 m·Myr^{-1} the TCN concentration acquired by grains after detachment from bedrock does not exceed 10% of the total TCN concentration acquired by the grains. Thus, the usual assumption in detrital thermochronology that the lag time (i.e., the difference between the stratigraphic age of the sediment from which the sample was collected and the sample's cooling age − Brandon and Vance, 1992) is short is justified. This assumption is also logically reasonable for the higher temperature thermochronometers for which closure temperatures are high and exhumation 'travel' times are long, relative to the post-detachment travel time through the catchment; the assumption of short lag times probably needs more rigorous justification for low-temperature detrital thermochronology. In any event, the back-

ground rate of exhumation indicated by low-temperature detrital thermochronology can be used to generate TCN concentrations during the last 2m of that exhumation and these can be then checked against the TCN concentration frequency distribution to test for substantial post-detachment acquisition, thereby providing a measure of lag time.

Acknowledgements

Codilean was funded by a University of Glasgow Postgraduate Scholarship and a Universities-UK Overseas Research Scholarships award. Valuable and constructive comments by Tibor Dunai and an anonymous reviewer are gratefully acknowledged. Discussions with John Jansen contributed to the improvement of an earlier version of the manuscript. The Scottish Universities Environmental Research Centre (SUERC) is supported by the Scottish Universities Consortium.

References

Ahnert F. 1970. Functional relationships between denudation, relief and uplift in large midlatitude drainage basins. *American Journal of Science* **268**: 243–263.

Beaumont C, Fullsack P, Hamilton J. 1992. Erosional control of active compresional orogens. In McClay K (ed.) *Thrust tectonics*. Chapman, London, 1–18.

Becker T, Ahrendt H, Weber K. 1994. The geological history of the Pre-Damara Gaub Valley Formation and the Weener Igneous Complex in the vicinity of Gamsberg. *Communications of the Geological Survey of Namibia* **9**: 79–91.

Becker T, Hansen BT, Weber K, Wiegand B. 1996. U-Pb and Rb-Sr isotopic data for the Moorivier Complex, Weener Igneous Suite and Gaub Valley Formation (Rehoboth Sequence) in the Nauchas area and their significance for Paleoproterozoic crustal evolution in Namibia. *Communications of the Geological Survey of Namibia* **11**: 31–46.

Bierman PR. 1994. Using in situ produced cosmogenic isotopes to estimate rates of landscape evolution: A review from the geomorphic perspective. *Journal of Geophysical Research* **99**: 13885–13896.

Bierman PR, Caffee MW. 2001. Slow rates of rock surface erosion and sediment production across the Namib Desert and Escarpment, Southern Africa. *American Journal of Science* **301**: 326–358. doi:10.2475/ajs.301.4-5.326.

Bierman PR, Nichols KK. 2004. Rock to sediment - slope to sea with ^{10}Be - rates of landscape change. *Annual Review of Earth and Planetary Sciences* **32**: 215–255. doi: 10.1146/annurev.earth.32.101802.120539.

Bishop P. 2007. Long-term landscape evolution: linking tectonics and surface processes. *Earth Surface Processes and Landforms* **32**: 329–365. doi:10.1002/esp.1493.

Brandon MT, Vance JA. 1992. New statistical methods for analysis of fission-track grain-age distributions with applications to detrital zircon ages from the Olympic subduction complex, western Washington State. *American Journal of Science* **292**: 565–636.

Carretier S, Regard V, Soual C. 2009. Theoretical cosmogenic nuclide concentration in river bed load clasts: Does it depend on clast size? *Quaternary Geochronology* **in press**. doi: 10.1016/j.quageo.2008.11.004.

Chang HH. 1988. *Fluvial processes in river engineering*. Wiley, New York.

Cockburn HAP, Brown RW, Summerfield MA, Seidl MA. 2000. Quantifying passive margin denudation and landscape development using a combined fission-track thermochronology and cosmogenic isotope analysis approach. *Earth and Planetary Science Letters* **179**: 429–435. doi:10.1016/S0012-821X(00)00144-8.

Codilean AT. 2006. Calculation of the cosmogenic nuclide production topographic shielding scaling factor for large areas using DEMs. *Earth Surface Processes and Landforms* **31**: 785–794.

Codilean AT, Bishop P, Stuart FM, Hoey TB, Fabel D, Freeman SPHT. 2008. Single-grain cosmogenic ^{21}Ne concentrations in fluvial sediments reveal spatially variable erosion rates. *Geology* **36**: 159–162. doi:10.1130/g24360a.1.

Crozier MJ, Vaughan EE, Tippett JM. 1990. Relative instability of colluvium-filled bedrock depressions. *Earth Surface Processes and Landforms* **15**: 329–339.

Desilets D, Zreda M. 2003. Spatial and temporal distribution of secondary cosmic-ray nucleon intensities and applications to in situ cosmogenic dating. *Earth and Planerary Science Letters* **206**: 21–42.

Dosseto A, Bourdon B, Turner SP. 2008. Uranium-series isotopes in river materials: Insights into the timescales of erosion and sediment transport. *Earth and Planetary Science Letters* **265**: 1–17.

Dunai TJ. 2000. Scaling factors for production rates of in situ produced cosmogenic nuclides: a critical reevaluation. *Earth and Planetary Science Letters* **176**: 157–169.

Dunne J, Elmore D, Muzikar P. 1999. Scaling factors for the rates of production of cosmogenic nuclides for geometric shielding and attenuation at depth on sloped surfaces. *Geomorphology* **27**: 3–11.

Ferguson RI, Bloomer DJ, Hoey TB, Werritty A. 2002. Mobility of river tracer pebbles over different timescales. *Water Resources Research* **38**: 1–8.

Gayer E, Mukhopadhyay S, Meade BJ. 2008. Spatial variability of erosion rates inferred from the frequency distribution of cosmogenic ^{3}He in olivines from Hawaiian river sediments. *Earth and Planerary Science Letters* **266**: 303–315.

Gosse JC, Phillips FM. 2001. Terrestrial in situ cosmogenic nuclides: theory and application. *Quaternary Science Reviews* **20**: 1475–1560.

Granger DE, Kirchner JW, Finkel RC. 1996. Spatially averaged long-term erosion rates measured from in situ-produced cosmogenic nuclides in alluvial sediment. *The Journal of Geology* **104**: 249–257.

Granger DE, Riebe CS. 2007. Cosmogenic nuclides in weathering and erosion. In Drever JI (ed.) *Surface and Ground Water, Weathering, and Soils*, *Treatise on Geochemistry*, volume 5. Elsevier, London.

Harrison CGA. 2000. What factors control mechanical erosion rates? *International Journal of Earth Sciences* **88**: 752–763. doi:10.1007/s005310050303.

Hassan MA, Church M. 1994. Vertical mixing of coarse particles in gravel bed rivers: A kinematic model. *Water Resources Research* **30**: 1173–1186. doi:10.1029/93WR03351.

Hoey TB, Bluck BJ. 1999. Identifying the controls over downstream fining of river gravels. *Journal of Sedimentary Research* **69**: 4–50.

Jenson SK, Domingue JO. 1988. Extracting topographic structure from digital elevation data for geographic information system analysis. *Photogrammetric Engineering and Remote Sensing* **54**: 593–600.

Kooi H, Beaumont C. 1994. Escarpment evolution on high-elevation rifted margins: insights derived from a surface process model that combines diffusion, advection, and reaction. *Journal of Geophysical Research* **99**: 191–209.

Krumbein WG. 1937. Sediments and exponential curves. *Journal of Geology* **45**: 577–601.

La Barbera P, Rosso R. 1989. On fractal dimension of stream networks. *Water Resources Research* **25**: 735–741.

Lal D. 1991. Cosmic ray labeling of erosion surfaces - In situ nuclide production rates and erosion models. *Earth and Planetary Science Letters* **104**: 424–439.

Libarkin JC, Quade J, Chase CG, Poths J, McIntosh W. 2002. Measurement of ancient cosmogenic ^{21}Ne in quartz from the 28 Ma Fish Canyon Tuff, Colorado. *Chemical Geology* **186**: 199–213.

Lifton NA, Bieber JW, Clem JM, Duldig ML, Evenson P, Humble JE, Pyle R. 2005. Addressing solar modulation and long-term uncertainties in scaling secondary cosmic rays for in situ cosmogenic nuclide applications. *Earth and Planerary Science Letters* **239**: 140–161.

Martin Y, Church M. 1997. Diffusion in landscape development models: on the nature of basic transport relations. *Earth Surface Processes and Landforms* **22**: 273–279.

Milliman JD, Syvitski JPM. 1992. Geomorphic / tectonic control of sediment discharge to the ocean. The importance of small mountainous rivers. *Journal of Geology* **100**: 525–544.

Molnar P. 2003. Geomorphology: Nature, nurture and landscape. *Nature* **426**: 612–614. doi: 10.1038/426612a.

Molnar P, England P. 1990. Late Cenozoic uplift of mountain ranges and global climate change: chicken or egg? *Nature* **346**: 29–34.

Montgomery DR, Foufoula-Georgiou E. 1993. Channel network source representation using digital elevation models. *Water Resources Research* **29**: 3925–3934.

Niedermann S. 2000. The ^{21}Ne production rate in quartz revisited. *Earth and Planetary Science Letters* **183**: 361–364. doi:10.1016/S0012-821X(00)00302-2.

Niedermann S. 2002. Cosmic-ray-produced noble gases in terrestrial rocks: Dating tools for surface processes. In Porcelli DP, Ballentine CJ, Wieler R (eds.) *Noble Gases*, *Reviews in Mineralogy and Geochemistry*, volume 47. 731–784.

Niemi NA, Oskin M, Burbank DW, Heimsath AM, Gabet EJ. 2005. Effects of bedrock landslides on cosmogenically determined erosion rates. *Earth and Planetary Science Letters* **237**: 480–498.

O'Callaghan JF, Mark DM. 1984. The extraction of drainage networks from digital elevation data. *Computer Vision, Graphics and Image Processing* **28**: 328–344.

Ollier CD, Marker ME. 1985. The Great Escarpment of southern Africa. *Zeitschrift für Geomorphologie N. F., Supplement Band* **54**: 37–56.

Oreskes N, Shrader-Frechette K, Belitz K. 1994. Verification, validation, and confirmation of numerical models in the Earth Sciences. *Science* **263**: 641–646.

Repka JL, Anderson RS, Finkel RC. 1997. Cosmogenic dating of fluvial terraces, Fremont River, Utah. *Earth and Planetary Science Letters* **152**: 59–73.

Stone JO. 2000. Air pressure and cosmogenic isotope production. *Journal of Geophysical Research* **105**: 23753–23760.

Summerfield MA. 1991. *Global geomorphology*. Longman, London.

Summerfield MA, Hulton NJ. 1994. Natural controls of fl uvial denudation rates in major world drainage basins. *Journal of Geophysical Research* **99**: 13871–13883. doi:10.1029/94JB00715.

Tarboton DG, Bras RL, Rodriguez-Iturbe I. 1988. The fractal nature of river networks. *Water Resources Research* **24**: 1317–1322.

van der Wateren FM, Dunai TJ. 2001. Late Neogene passive margin denudation history-cosmogenic isotope measurements from the central Namib desert. *Global and Planetary Change* **30**: 271–307. doi:10.1016/S0921-8181(01)00104-7.

von Blanckenburg F. 2005. The control mechanisms of erosion and weathering at basin scale from cosmogenic nuclides in river sediment. *Earth and Planetary Science Letters* **237**: 462–479.

Whipple KX, Tucker GE. 1999. Dynamics of the stream-power incision model: implications for height limits of mountain ranges, landscape response timescales, and research needs. *Journal of Geophysical Research* **104**: 661–674.

Ziegler URF, Stoessel GFU. 1993. *Age determinations in the Rehoboth Basement Inlier, Namibia*, *Geological Survey of Namibia Memoir*, volume 14.

Figure captions

1 Schematic representation of the pathways of two different sediment 'grains' from source to the location of sampling. The two grains originate from different locations with potentially very different elevations and erosion rates, and can spend different amounts of time at different elevations (and depths within the transport layer) while in transit. Thus, the final TCN concentration of a grain reflects its potentially unique history of erosion, transport and deposition. 27

2 Location map of the upper Gaub River catchment showing roads and tracks. 28

3 Morphology and geology of the upper Gaub River catchment. (A) Slope map calculated from the 90 m SRTM data. (D) Geological map of the study area. Data obtained from the Geological Survey of Namibia (http://www.mme.gov.na/gsn/). 29

4 Summary of the published TCN data. (A) Diagrammatic topographic profile across central-western Namibia (thick line) summarizing the TCN-based denudation rates of Bierman and Caffee (2001), Cockburn *et al.* (2000), Codilean *et al.* (2008) and van der Wateren and Dunai (2001) from 'spot' bedrock and clast samples (above the topographic profile) and amalgamated sediment samples (below the topographic profile). Rates inferred from cosmogenic ^{10}Be are given in normal typeface and those inferred from cosmogenic ^{21}Ne are given in italic. Bierman and Caffee's (2001) and Cockburn et al.'s (2000) rates have been recalculated using a sea level high latitude production rate for ^{10}Be of 5.1 ± 0.3 atoms$\cdot$g$^{-1}\cdot$yr^{-1} and scaling factors given by Stone (2000) and Codilean (2006). Original image courtesy of Roderick Brown. (B) Plot of ^{10}Be denudation rates obtained for Gaub sub-catchments by Bierman and Caffee (2001) and Codilean *et al.* (2008) versus area-weighted mean slopes of these subcatchments. Modified from Codilean *et al.* (2008). 30

5 Schematic representation of the pathway of a sediment grain from its source to the location of sampling showing the three conceptual domains used in the model: a bedrock domain, a hillslope domain, and a fluvial domain. The total ^{21}Ne$_c$ concentration acquired by a sediment grain depends upon (1) the elevation and bedrock erosion rate at its source location within the catchment, and (2) its pathway through the catchment and the time it spends at each elevation along this pathway. 31

6 Predicted $^{21}Ne_c$ concentration distributions for the upper Gaub River catchment for different numbers of grains in a sample. Denudation is taken to vary linearly with slope between 0.1 to 10 m·Myr^{-1}. Each grey line represents one predicted $^{21}Ne_c$ distribution and there are 1000 predicted $^{21}Ne_c$ distributions in each plot. Note how the envelopes of predicted $^{21}Ne_c$ concentration distributions become narrower as the number of grains in a sample increases. 32

7 Cumulative frequency distribution plots comparing Codilean et al.'s (2008) $^{21}Ne_c$ concentrations measured in pebbles (circles) with predicted $^{21}Ne_c$ concentration distribution envelopes obtained for the upper Gaub River catchment for different ranges of bedrock erosion rates. The envelopes are based on 1000 predicted $^{21}Ne_c$ concentration distributions, each obtained by sampling 32 grains. In each plot, 95% of the predicted $^{21}Ne_c$ concentration distributions lie within the grey areas and 50% lie within the dark-grey areas. Insets show frequency distribution plots of the number of $^{21}Ne_c$ distributions along transects A, B, and C. 33

8 Results of the simulations exploring the sensitivity of the $^{21}Ne_c$ concentration distribution to the assumptions that are made about the spatial pattern of denudation in the Gaub. (A) $^{21}Ne_c$ concentration distributions for the upper Gaub River catchment (grey lines) obtained assuming spatially uniform bedrock erosion throughout the catchment. Note how the form of the predicted envelope of $^{21}Ne_c$ concentration distributions mirrors the form of hypsometric curve. The displacement to the left of the $^{21}Ne_c$ envelope results from the non-linear dependence of TCN production rates on elevation. (B) Cumulative frequency distribution plots comparing Codilean et al.'s (2008) $^{21}Ne_c$ concentrations (circles) with predicted $^{21}Ne_c$ concentration distributions (grey lines) obtained for (B1) bedrock erosion assumed to be spatially variable as a linear function of slope, and for (B2) bedrock erosion assumed to be spatially variable as a second order power function of slope. For both (B1) and (B2) erosion is taken to vary between 0.1 and 10 m·Myr^{-1}. Each grey line represents one predicted $^{21}Ne_c$ distribution and was obtained by sampling 32 sediment grains. There are 1000 predicted $^{21}Ne_c$ concentration distributions in each plot. 34

9 Schematic representation of the two end-member cases that may be identified in accounting for the $^{21}Ne_c$ concentrations in the sediment leaving a catchment. See text for more details. 35

10 Normalised $^{21}Ne_c$ concentration distributions obtained for the Gaub for different values of the diffusion coefficient (K_D) for two hypothetical scenarios: (A) spatially uniform bedrock erosion at 10 m·Myr^{-1}, and (B) spatially uniform bedrock erosion at 100 m·Myr^{-1}. Once the sediment residence times become long enough for the post-detachment $^{21}Ne_c$ concentrations in the grains to exceed the $^{21}Ne_c$ concentrations acquired prior to detachment from the bedrock, the $^{21}Ne_c$ 'signal' in the grains becomes 'post-detachment dominated' and the $^{21}Ne_c$ concentration distributions cease to be primarily determined by catchment hypsometry. Each line represents one model run and is obtained by sampling 10^5 sediment grains. 36

11 Frequency distribution plot of the distances from each 'hillslope' DEM cell to the nearest 'channel' DEM cell for the upper Gaub River catchment. Obtained using 30 m ASTER DEM. 37

12 Results of the simulations exploring the sensitivity of the $^{21}Ne_c$ concentration distribution to the assumptions that are made about the importance of lithology in controlling the rate of erosion and the quartz flux in the Gaub. $\varepsilon 1$ and $\varepsilon 2$: the erosion rates in zone 1 and zone 2, respectively; z1 and z2: the proportions of quartz contributed by zone 1 and zone 2, respectively. (A1) Map showing the two principal lithological zones: zone 1 − predominantly quartzite, and zone 2 − predominantly granite. (A2) Normalised $^{21}Ne_c$ concentration distributions for the upper Gaub River catchment obtained assuming uniform bedrock erosion rates in the two zones. (A3) Normalised $^{21}Ne_c$ concentration distributions for the upper Gaub River catchment obtained assuming that the bedrock erosion rate in zone 1 is 20% greater than that in zone 2. (B1) Map showing the two new zones: zone 1 − steep escarpment area plus coastal plain, and zone 2 − upland plateau. (B2) Normalised $^{21}Ne_c$ concentration distributions for the upper Gaub River catchment obtained assuming uniform bedrock erosion rates in the two zones. (B3) Normalised $^{21}Ne_c$ concentration distributions for the upper Gaub River catchment obtained assuming that the bedrock erosion rate in zone 1 is 20% greater than that in zone 2. (B4) Normalised $^{21}Ne_c$ concentration distributions for the upper Gaub River catchment obtained for various differences in the bedrock erosion rates of the two zones. Each line represents one model run and is obtained by sampling 10^5 sediment grains. Negligible post-detachment $^{21}Ne_c$ acquisition is assumed. 38

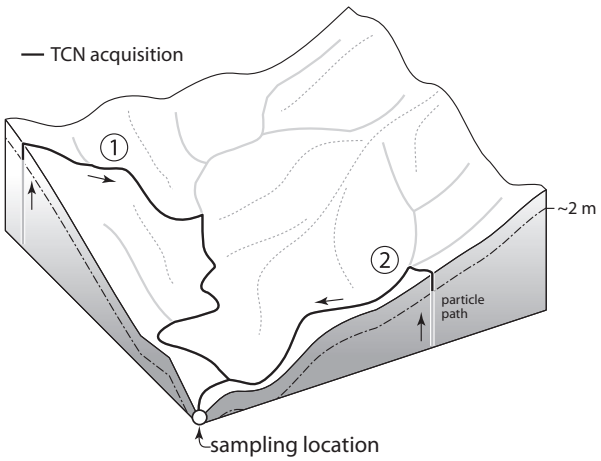

Figure 1

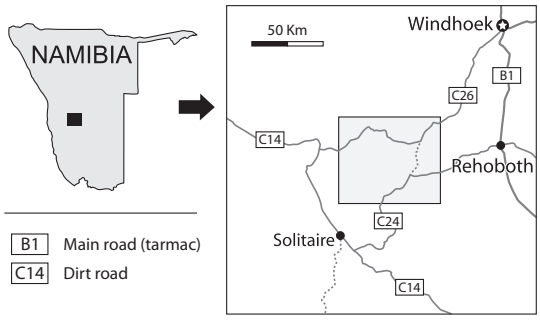
NAMIBIA
B1 Main road (tarmac)
C14 Dirt road
50 Km
Windhoek
B1
C26
C14
Rehoboth
C24
Solitaire
C14

Figure 2

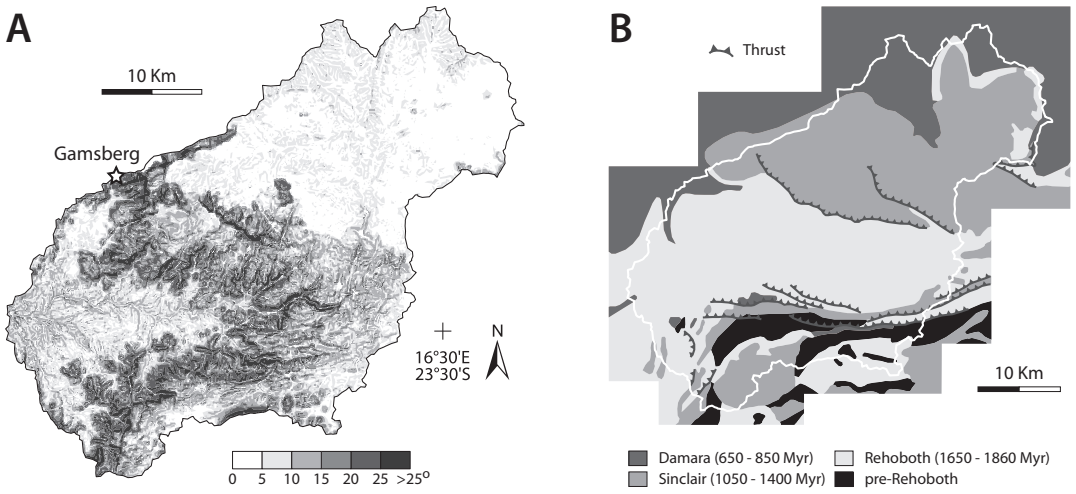
A
10 Km
Gamsberg
16°30'E
23°30'S
N
0 5 10 15 20 25 >25°
B
Thrust
10 Km
Damara (650 - 850 Myr)
Sinclair (1050 - 1400 Myr)
Rehoboth (1650 - 1860 Myr)
pre-Rehoboth

Figure 3

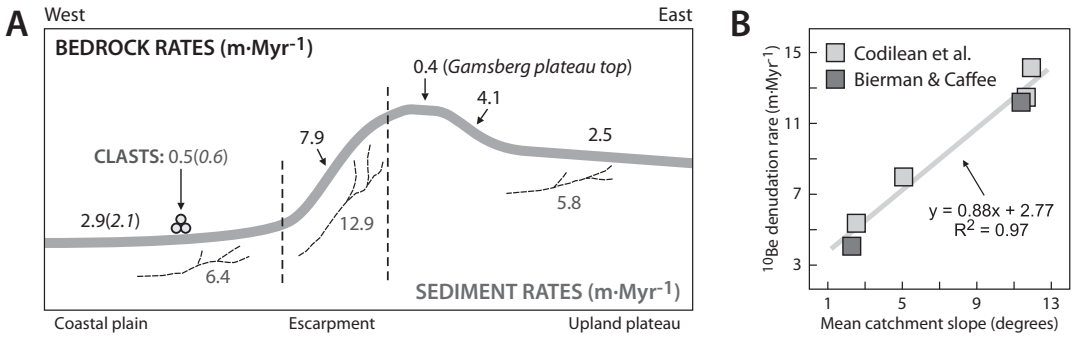
A
West
East
BEDROCK RATES (m·Myr⁻¹)
0.4 (Gamsberg plateau top)
4.1
7.9
2.5
CLASTS: 0.5(0.6)
2.9(2.1)
12.9
5.8
6.4
SEDIMENT RATES (m·Myr⁻¹)
Coastal plain
Escarpment
Upland plateau
B
Codilean et al.
Bierman & Caffee
y = 0.88x + 2.77
R2 = 0.97
10Be denudation rare (m·Myr⁻¹)
15
11
7
3
1
5
9
13
Mean catchment slope (degrees)

Figure 4

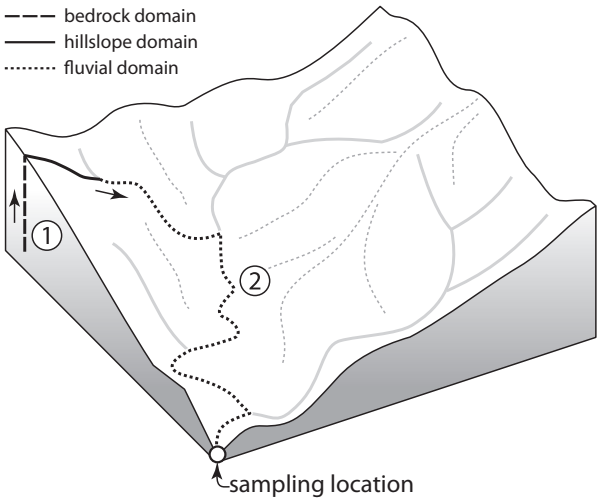
bedrock domain
hillslope domain
fluvial domain
1
2
sampling location

Figure 5

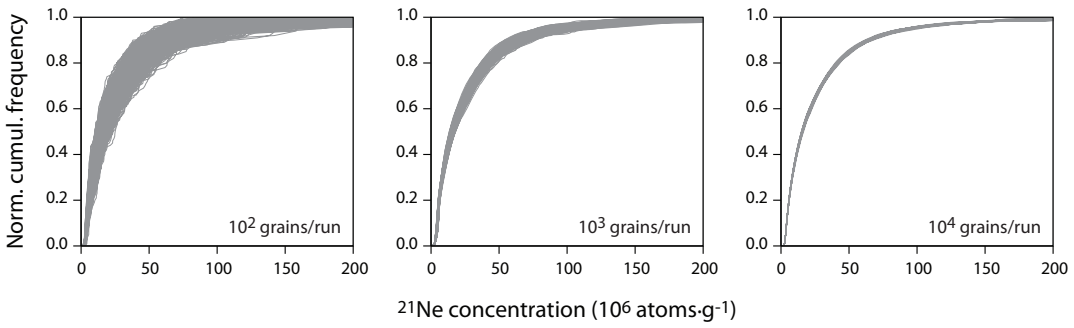
Norm. cumul. frequency
1.0
0.8
0.6
0.4
0.2
0.0
0
50
100
150
200
10^2 grains/run
10^3 grains/run
10^4 grains/run
21Ne concentration (10^6 atoms·g^-1)

Figure 6

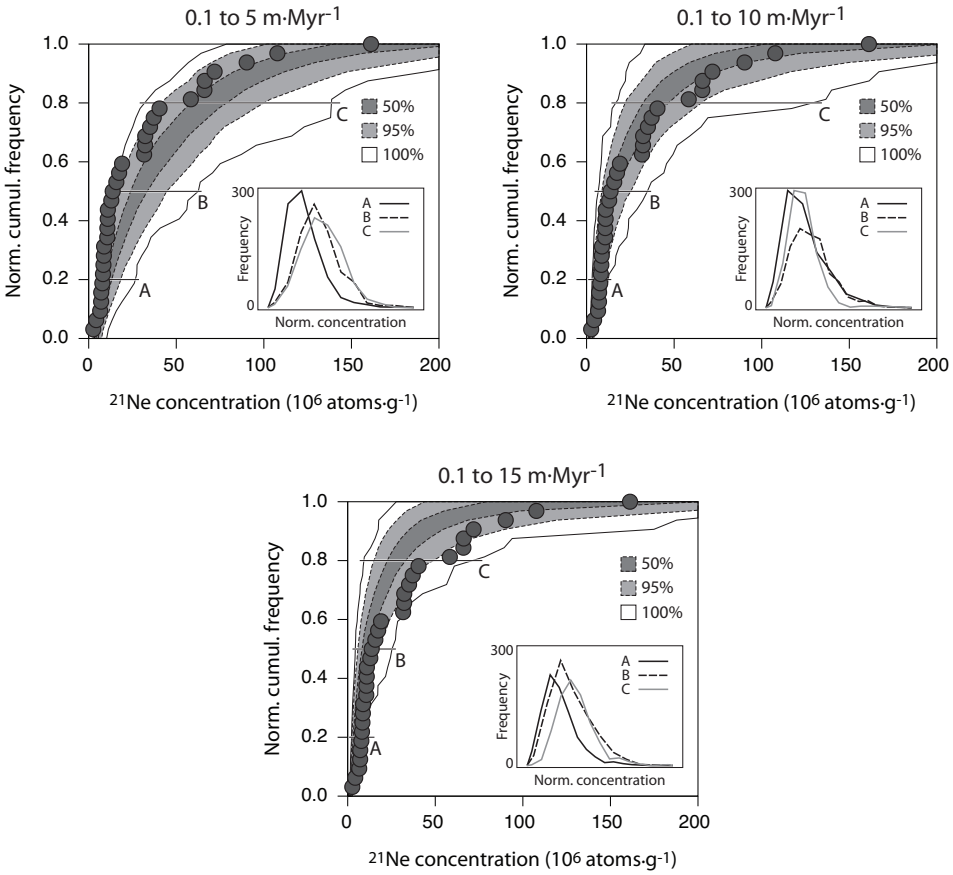
0.1 to 5 m·Myr-1
0.1 to 10 m·Myr-1
0.1 to 15 m·Myr-1
Norm. cumul. frequency
21Ne concentration (10⁶ atoms·g-1)
50%
95%
100%
A
B
C
Frequency
Norm. concentration

Figure 7

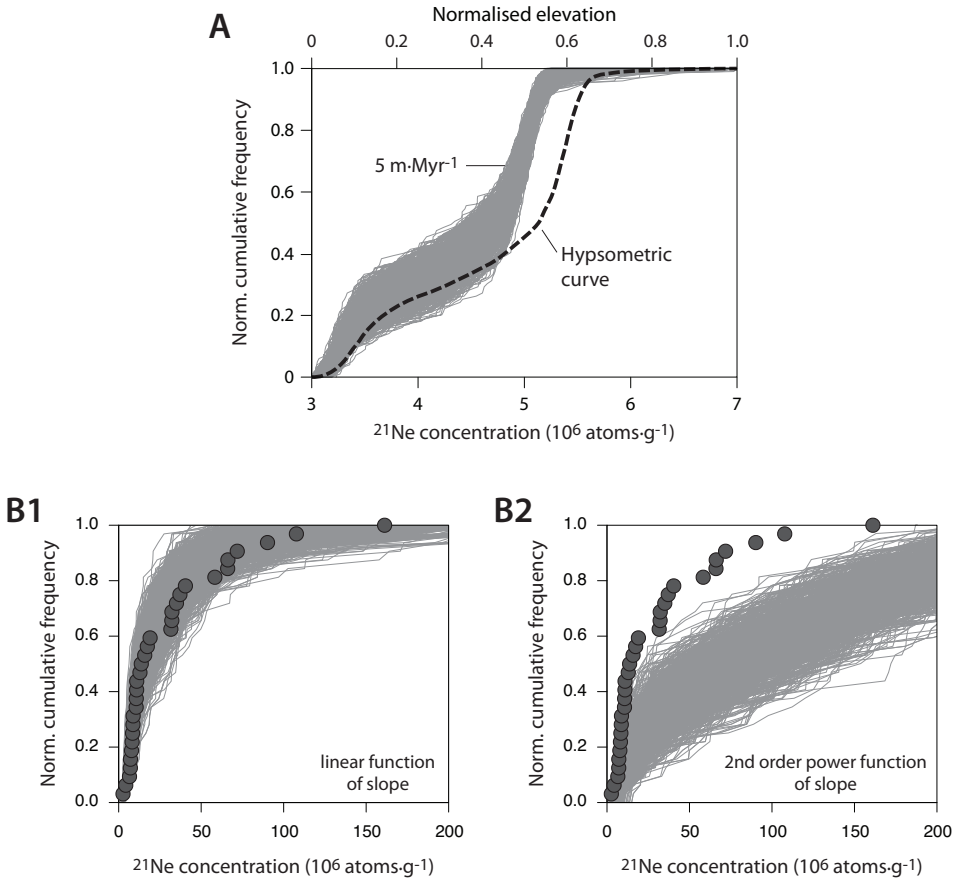
A
Normalised elevation
0
0.2
0.4
0.6
0.8
1.0
Norm. cumulative frequency
5 m·Myr-1
Hypsometric curve
21Ne concentration (10⁶ atoms·g-1)
B1
linear function of slope
B2
2nd order power function of slope

Figure 8

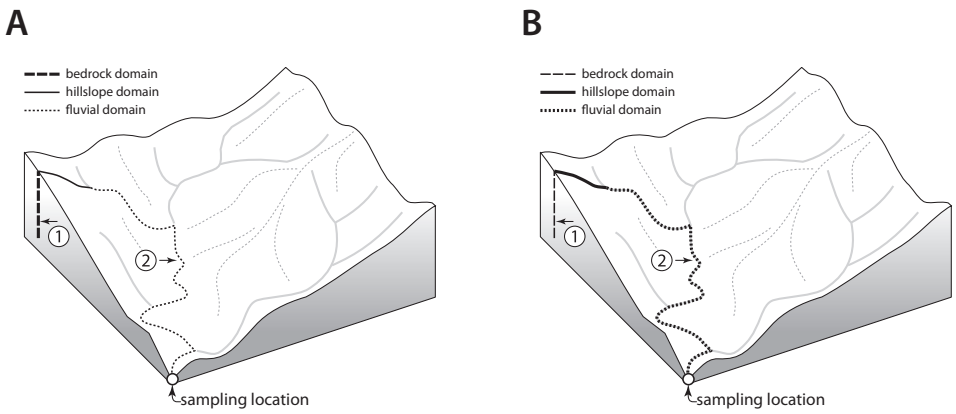
A
bedrock domain
hillslope domain
fluvial domain
1
2
sampling location
Pre-detachment dominated
$^{21}Ne_C$ acquired during 1 >> 2
B
bedrock domain
hillslope domain
fluvial domain
1
2
sampling location
Post-detachment dominated
$^{21}Ne_C$ acquired during 1 << 2

Figure 9

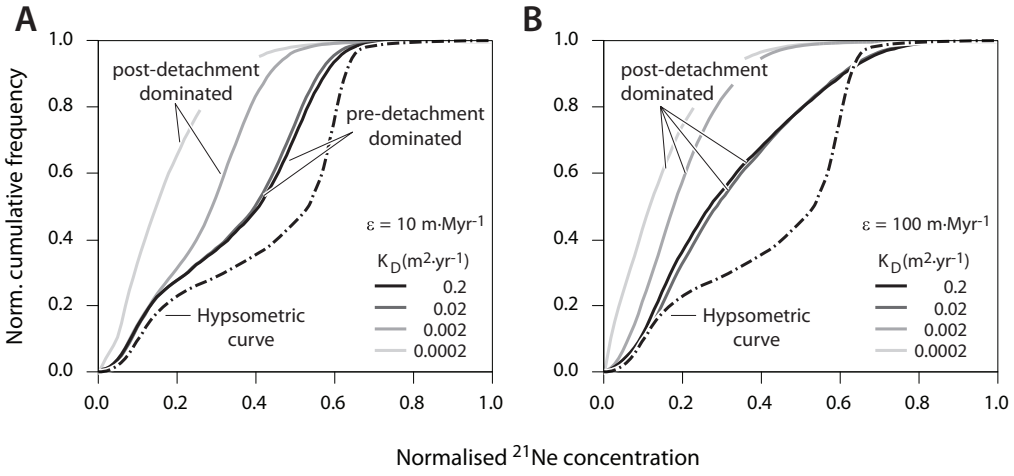
A
B
1.0
0.8
0.6
0.4
0.2
0.0
0.0
0.2
0.4
0.6
0.8
1.0
Norm. cumulative frequency
post-detachment dominated
pre-detachment dominated
Hypsometric curve
ε = 10 m·Myr-1
ε = 100 m·Myr-1
K_D(m2·yr-1)
0.2
0.02
0.002
0.0002
Normalised 21Ne concentration

Figure 10

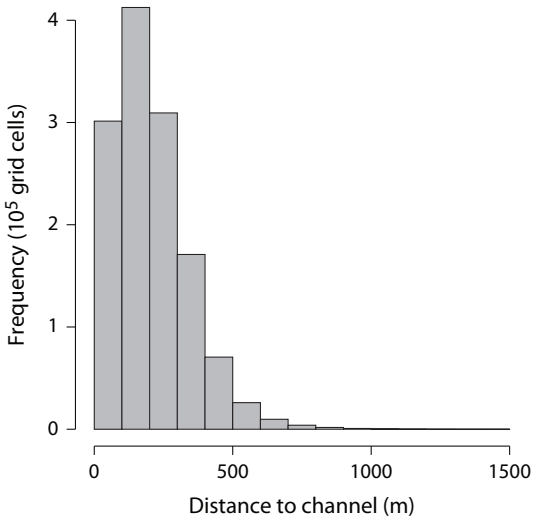
Frequency (10^5 grid cells)
0
1
2
3
4
0
500
1000
1500
Distance to channel (m)

Figure 11

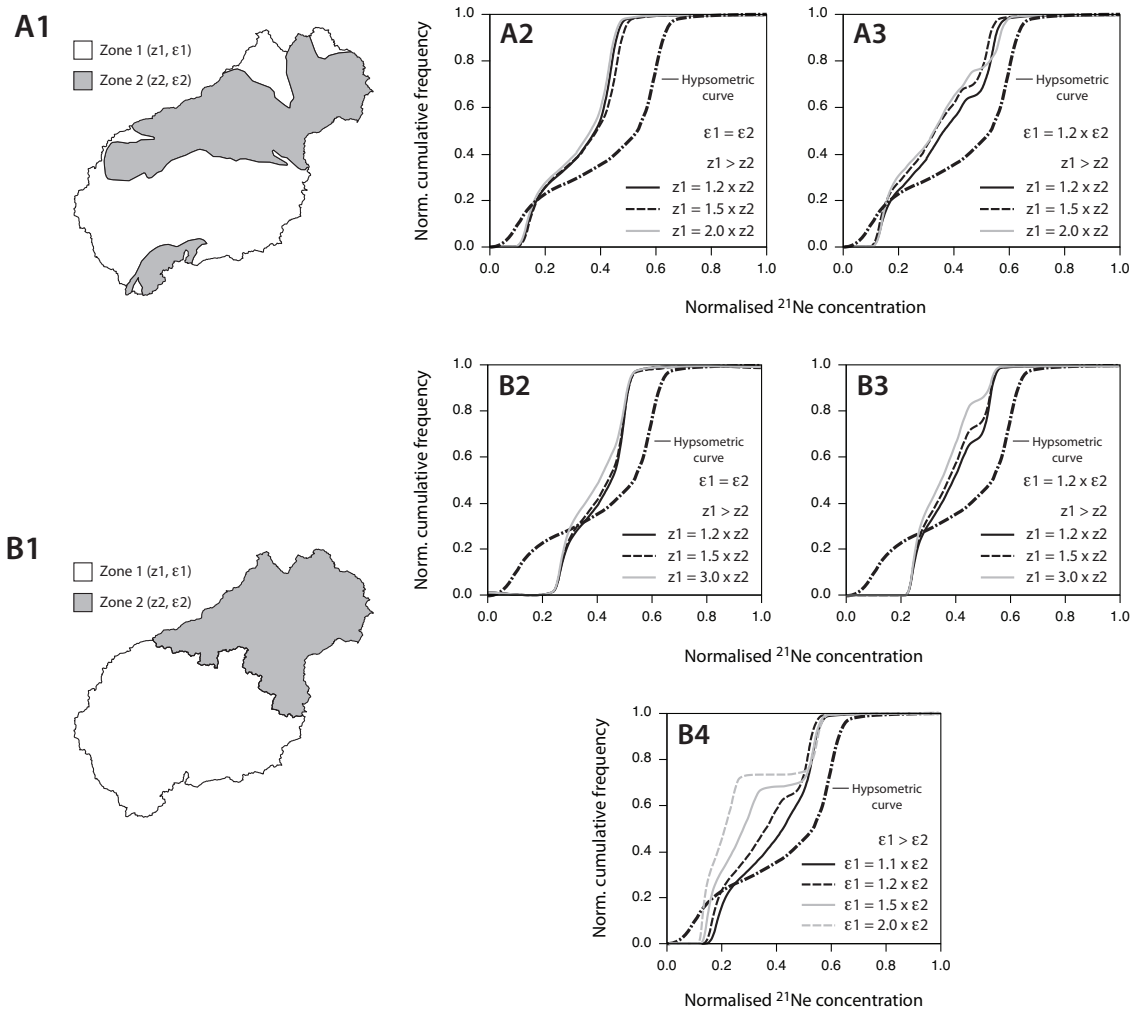
A1
Zone 1 (z1, ε1)
Zone 2 (z2, ε2)
A2
A3
Hypsometric curve
ε1 = ε2
z1 > z2
z1 = 1.2 x z2
z1 = 1.5 x z2
z1 = 2.0 x z2
ε1 = 1.2 x ε2
Norm. cumulative frequency
Normalised 21Ne concentration
B1
Zone 1 (z1, ε1)
Zone 2 (z2, ε2)
B2
B3
z1 = 3.0 x z2
B4
ε1 > ε2
ε1 = 1.1 x ε2
ε1 = 1.2 x ε2
ε1 = 1.5 x ε2
ε1 = 2.0 x ε2

Figure 12